



Theoretical Analysis of Collective Stochastic Resonance with Population Heterogeneity

Tohru Sahashi[†], Akira Utagawa, Tetsuya Asai, and Yoshihito Amemiya

Graduate School of Information Science and Technology, Hokkaido University.

Kita 14, Nishi9, Kita-ku, Sapporo, 060-0814 Japan.

Phone: +81-11-706-7147, Fax: +81-11-706-7890

[†] email: sahashi@lalsie.ist.hokudai.ac.jp

Abstract

We proposed a retinomorphic neural network model in [1] and through simulations observed a new type of stochastic resonance where nonzero receptive field size has maximal correlation between the subthreshold inputs and outputs. We theoretically prove that this kind of stochastic resonance occurs in the retinomorphic model proposed in [1] in this paper. We discuss several constraints to derive a theoretical equation that explains this phenomenon and show that not only certain noises intensity provide the optimal performance of signal detection but also nonzero receptive field size is a factor as well.

1. Introduction

Stochastic resonance (SR) has recently been spotlighted in the field of electrical engineering, which is motivated by a wide variety of sensing applications for detecting weak signals. Among the SR applications, night-scope (dark) image sensing [2] seems to be particularly promising in semiconductor research fields because present image sensors use very precise (and thus expensive) devices for photon sensing or counting. However, SR would be useful only for detecting dark light in a single photosensor, but not for canceling mismatches between the photosensors in the sensor array (image sensor).

Recently, Funke *et al.* reported that a visual pathway in a cat's primary visual cortex optimally used a SR-like process to improve signal detection while preventing spurious noise-induced activity and keeping the SNR high [3]. Although the mechanism is still unclear, one may assume that i) SR without optimal tuning of the noise intensities [4] underlies the fundamental mechanism and ii) the visual pathway from the photoreceptors to the cortical neurons may cause an extremely large receptive field (RF). Under these assumptions, we consider a relatively short pathway, i.e., from the photoreceptors to the subsequent layer in the vertebrate retinae, and propose a retinomorphic neural network that has parallel SR components with variable RFs.

Motivated by the results obtained by Funke *et al.* [3], we

proposed a simple retinomorphic neural network consisting of nonidentical photoreceptors for the development of image sensor systems [1]. We used numerical simulations to observe a new class of stochastic resonance among the nonidentical pixels. We calculated the correlation values between the optical inputs and outputs as a function of the receptive field (RF) size and intensities of the random components in the photoreceptors and the McCulloch-Pitts neurons (thresholds elements). We then found the optimal nonzero sizes of the RF as well as the optimal noise intensities of the neurons under the nonidentical photoreceptors.

We provide a theoretical analysis for this neural network model in this paper to confirm that setting the receptive field size to an optimal value improves the performance when there are spatial noises caused by the photodetectors in this model. In Sec. 2, a structure of the neural network model is briefly explained. In addition, a theoretical analysis of this network is presented in Sec. 3. In Sec. 4, our simulation and theoretical results are compared.

2. Retinomorphic neural network model

Let us consider the 1-D network shown in Fig. 1 where the optical input distribution is represented by $I(x)$. The output distribution of the photoreceptors is defined by $I(x) + \delta(x)$, where $\delta(x)$ represents the spatial random noise (pixel variations) given by $m \cdot N(0, 1)$ [$N(0, 1)$ is the Gaussian noise with a zero mean and a unity standard deviation]. The input to the neurons via the local synaptic layer between the photoreceptors and the neurons is then defined by

$$R(x) = \int (I(y) + \delta(y)) \cdot g(y - x) dy \equiv (I + \delta) * g, \quad (1)$$

$$g(x) = \frac{1}{\sqrt{2\pi}\sigma} \exp\left[-\frac{x^2}{2\sigma^2}\right], \quad (2)$$

where σ represents the receptive field (RF) size. The output distribution of the neurons is defined by $V(x) = H(R(x) - \xi(t))$, where $H(\cdot)$ represents a step function and $\xi(t)$ is the temporal random noise given by $A \cdot N(0, 1) + \theta$ (A : noise intensity, θ : mean threshold). The final output via the local synaptic

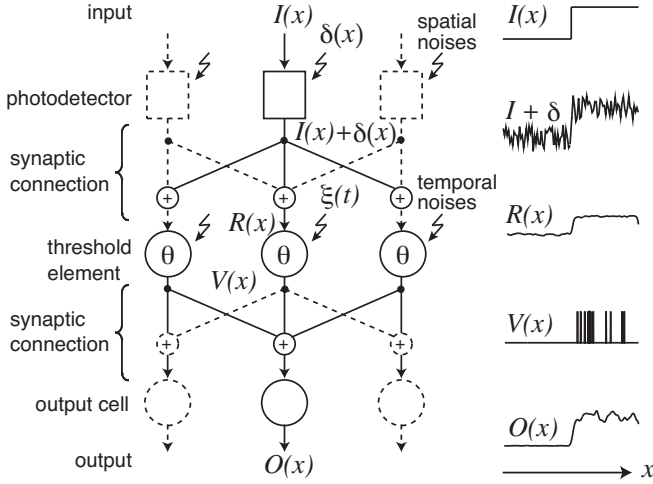


Figure 1: Receptive field model proposed in [1]. The squares represent photoreceptors with spatial noise δ receiving optical input $I(x)$, The circles in the middle of the figure represents threshold elements with a threshold θ receiving temporal noises $\xi(t)$, and the circles at the bottom of the figure represent the final cells that produce outputs $O(x)$. The input of the threshold elements is given by $(I + \xi) * g$ and the input of the final cells is given by $V * g$, where g is a Gaussian distribution function whose standard deviation is σ and its average is 0.

layer between the neurons and the output cells is then given by $O(x) = V * g$. The optical input $I(x)$ is set to $S \cdot H(x)$, where S represents the strength of the input. With this model, we analyze the SR behaviors by systematically changing m (spatial randomness), σ (RF size), and A (temporal randomness that is necessary for SR).

3. Theoretical Analysis

We first consider the dependence of the output $O(x)$ on the noise intensity A when RF size σ is small, i.e., $g(x)$ is the delta function and the spatial noises of the photodetectors m are 0. In this case, commonly-known stochastic resonance would be observed in this model where the subthreshold inputs $I(x)$ that are given to the threshold elements were amplified by applying temporal noises $\xi(t)$ to the threshold elements. Here, we consider the mean squared error E between optical input $I(x)$ and the time-averaged output $\langle O(x) \rangle$ to evaluate the characteristics of our model. We define the mean squared error E in the model as

$$E = \frac{1}{X} \int_{-X/2}^{X/2} (\langle O \rangle - I(x))^2 dx, \quad (3)$$

where X represents the domains of $I(x)$ and $O(x)$. As described in Sec. 2, the output of the threshold elements $V(x)$

is $(I + \delta) * g(x)$ and the output of the final cells $O(x)$ is $V(x) * g(x)$. The threshold elements receiving temporal noises may respond to the subthreshold inputs if the sum of the inputs and the temporal noises exceeds the threshold values of the threshold elements. The response strongly depends on the noise sequences, i.e., the neuron's output would be 1-bit temporal random sequences (time varying sequences of 0 and 1). When the output of the threshold elements $V(x)$ is averaged over time; the averaged value $\langle V \rangle$ converges to static values. By considering the effect of time averaging, the equation for the mean squared error between $I(x)$ and $\langle O \rangle$ is quite simple. If noises are applied to the neurons with an optimal intensity, the time-averaged output of the threshold elements $\langle V \rangle$ converges to the subthreshold input, i.e., $\langle V \rangle$ is strongly correlated with the input. Thus, the output of the threshold elements can be represented by its input. We used uniform noises for simplicity reasons, rather than Gaussian noises which often yields complex equations. When the noises has a uniform distribution (range of value is given by $[-A' : A']$), the output is equal to its input at an optimal intensity. $\langle V \rangle$ is equal to $\langle R \rangle$ which represents the input of the threshold elements because the threshold elements simply transfer their inputs $\langle R \rangle$ to their outputs $\langle V \rangle$ when optimal noises are applied. Therefore,

$$\langle O \rangle = \langle V \rangle * g = \langle R \rangle * g = ((I + \delta) * g) * g. \quad (4)$$

By factorizing the equation, we acquire

$$\langle O \rangle = ((I * g) * g) + ((\delta * g) * g). \quad (5)$$

$g * g$ ($\equiv g'$) is the convolutions of two Gaussian distribution functions. g' follows a Gaussian distribution function whose standard deviation is $\sqrt{2}\sigma$. Therefore, E can be rewritten as

$$E = \frac{1}{X} \int_{-X/2}^{X/2} ((I * g') + (\delta * g') - I(x))^2 dx. \quad (6)$$

We define E_0 , E_1 and E_2 as follows:

$$E_0 = \frac{1}{X} \int_{-X/2}^{X/2} ((I * g') - I(x)) \cdot (\delta * g') dx \quad (7)$$

$$E_1 = \frac{1}{X} \int_{-X/2}^{X/2} ((I * g') - I(x))^2 dx, \quad (8)$$

$$E_2 = \frac{1}{X} \int_{-X/2}^{X/2} ((\delta * g'))^2 dx. \quad (9)$$

By using these equations, E yields

$$E = E_1 + 2 \cdot E_0 + E_2. \quad (10)$$

$E_0 \approx 0$ because $((I * g') - I(x))$ and $\delta * g'$ are uncorrelated. Therefore $E \approx E_1 + E_2$. This implies that E can be obtained by independently deriving E_1 and E_2 .

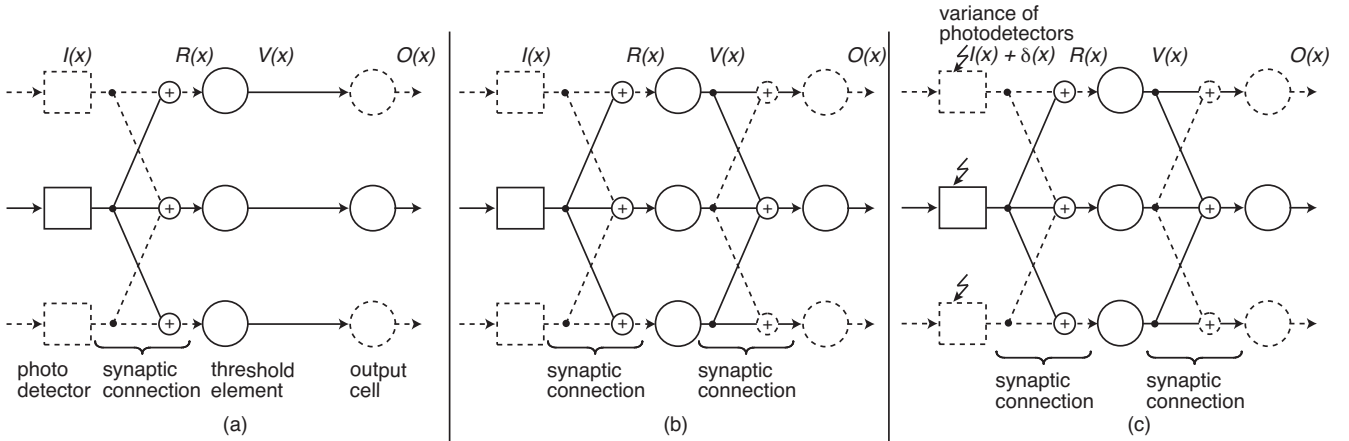


Figure 2: Receptive field model: (a) having local layer between photodetectors and threshold elements, (b) having local synaptic layers between photodetectors and threshold elements and between threshold elements and output cells, and (c) having local synaptic layers between nonidentical photodetectors and threshold elements and between threshold elements and output cells

Here, we explain the dependence of E on the receptive field size σ . Figure 2(a) represents a model where the local synaptic layers between the threshold elements and the output cell are removed ($O(x) = R(x)$) and m is 0. In this case, the E between $I(x)$ and $\langle O \rangle$ is given by

$$E = \frac{1}{X} \int_{-X/2}^{X/2} (R(x) - I(x))^2 dx, \quad (11)$$

$$= \frac{1}{X} \int_{-X/2}^{X/2} ((I * g) - I(x))^2 dx. \quad (12)$$

$I(x)$ is 0 when $x < 0$, whereas $I(x)$ is S when $x > 0$, as described in Sec. 2, and then

$$(I * g) = S \int_0^{X/2} g(y - x) dy. \quad (13)$$

The integral of the Gaussian distribution is given by using an error function, and we thus obtain

$$(I * g) = \frac{S}{2} \left\{ \operatorname{erf} \left(\frac{X/2 - x}{\sqrt{2}\sigma} \right) - \operatorname{erf} \left(\frac{x}{\sqrt{2}\sigma} \right) \right\} \quad (14)$$

When X is much larger than σ ,

$$(I * g) \approx \frac{S}{2} \left(1 - \operatorname{erf} \left(\frac{x}{\sqrt{2}\sigma} \right) \right). \quad (15)$$

By substituting this equation into Eqn. 12, we can obtain

$$E = \frac{1}{X} \int_{-X/2}^{X/2} \left(I(x) - \frac{S}{2} \left(1 - \operatorname{erf} \left(\frac{x}{\sqrt{2}\sigma} \right) \right) \right)^2 dx, \quad (16)$$

$$= \frac{S^2}{2X} \int_0^{X/2} \left(1 - \operatorname{erf} \left(\frac{x}{\sqrt{2}\sigma} \right) \right)^2 dx. \quad (17)$$

We used the symmetric characteristic of E to obtain the equation mentioned above.

When two synaptic layers are used as shown in Fig. 2 (b), the error in this case can simply be obtained by replacing σ with $\sqrt{2}\sigma$ in Eqn. 17 because the difference between Fig. 2 (a) and (b) is only the variance of the distribution. Therefore, we obtain

$$E = \frac{S^2}{2X} \int_0^{X/2} \left(1 - \operatorname{erf} \left(\frac{x}{2\sigma} \right) \right)^2 dx = E_1. \quad (18)$$

The dependence of E on m is explained here. When all the synaptic layers are removed and $\delta \neq 0$,

$$\langle O \rangle = \langle V \rangle = \langle R \rangle = I + \delta. \quad (19)$$

Then, E can simply be expressed by

$$E = \frac{1}{X} \int_{-X/2}^{X/2} (\langle O \rangle - I(x))^2 dx = \frac{1}{X} \int_{-X/2}^{X/2} \delta^2 dx, \quad (20)$$

representing that E is proportional to the spatial noises.

Figure 2 (c) shows a model with the spatial noises of the photodetectors. Here, we consider the error caused by δ given by

$$E_2 = \frac{1}{X} \int_{-X/2}^{X/2} (\delta * g')^2 dx. \quad (21)$$

At first, we obtain the equations for $\delta * g'$. It is usually impossible to represent stochastic variables with deterministic variables. However, when X is large enough, only the statistical characteristics of δ are required; we don't have to directly deal with random variables. In the actual calculation, we consider $(I + \delta) * g$ instead of only $\delta * g$. The $(I + \delta) * g$ in Fig.3(a)

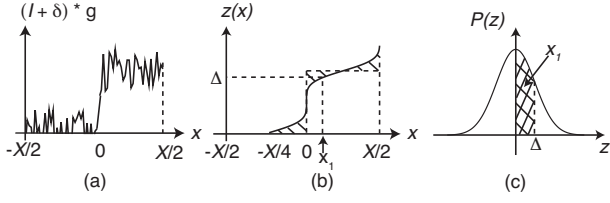


Figure 3: 1-D plot for $O(x)$ when spatial noises of photodetectors are given: (a) Distribution of $(I+\delta)*g$, (b) Distribution of $z(x)$ (obtained by arranging $(I+\delta)*g$ in ascending order), and (c) Probability distribution of z

was sorted in ascending order as shown in Fig. 3(b) for convenience. The resulting curve is defined as $z(x)$ and is plotted with a solid curve in Fig. 3(c). As indicated by the area filled with oblique lines in Fig. 3 (b) E_2 is give by

$$E_2 = \frac{1}{X} \int_{-X/2}^{X/2} (z(x) - I(x))^2 dx = \frac{3}{X} \int_{-X/4}^0 z(x)^2 dx. \quad (22)$$

It should be noted that $(I+\delta)*g(\equiv z(x))$ is always positive because the applied noises have an optimal intensity. Figure 3 (c) shows the probability distribution of z . Here we consider $z(x_1) = \Delta$, as shown in Fig. 3 (b). Then, we obtain

$$x_1 = \frac{X}{2} \int_0^\Delta P(z) dz = \frac{X}{4} \operatorname{erf} \left(\frac{\Delta}{\sqrt{2}\sigma_o} \right), \quad (23)$$

where σ_o is defined as the standard deviation of $O(x)$. We obtain $\Delta = \sqrt{2}\sigma_o \operatorname{erf}^{-1}(4x_1/X)$ by inverting the equation. Δ represents $z(x)$, and thus, by replacing $z(x)$ with Δ in Eqn. 22, we can obtain

$$E_2 = \frac{3}{X} \int_{-X/4}^0 \left(\sqrt{2}\sigma_o \operatorname{erf}^{-1} \left(\frac{4x}{X} \right) \right)^2 dx \quad (24)$$

$$= \frac{3}{X} \cdot 2\sigma_o^2 \int_{-X/4}^0 \left(\operatorname{erf}^{-1} \left(\frac{4x}{X} \right) \right)^2 dx, \quad (25)$$

where σ_o^2 is given by $\sigma_o^2 = m^2/(2\sqrt{\pi}\sigma)$. We obtained the equations for E_1 and E_2 from Eqns. 18 and 25.

4. Comparison of simulation and theoretical results

Here, we compare the simulation and theoretical results given in the previous section. The noises that were applied had an optimal intensity ($A' = 0.5$), an input amplitude of 0.3 ($S = 0.3$), the spatial noises of the photodetectors σ were set to 0.06, the number of pixel N was set to 500, T was set to 1000, and the threshold of threshold elements was set to 0.5. Figure 4 shows the dependence of E on σ for the numerical simulation (dotted curve) and the theoretical equation (solid curve). E_1 and E_2 were also plotted. As shown in this figure,

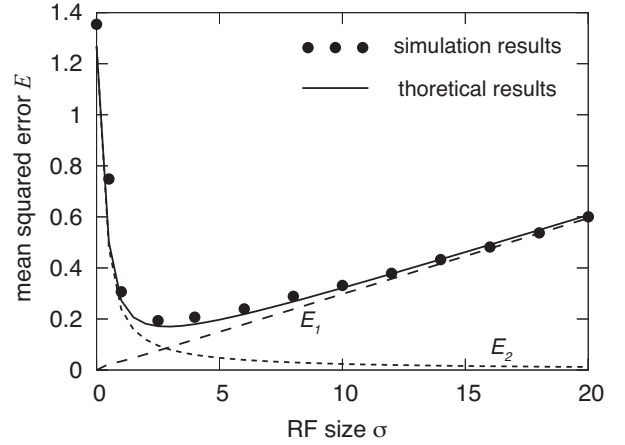


Figure 4: Comparison between theoretical error (solid curve) and one obtained by simulations (dotted curve). The errors from the receptive field (E_1) and spatial noises (E_2) are also plotted

the theoretical results quantitatively matched with the simulation results. The E_2 plots shows that the error due to spatial noises was dominant when RF size was small while E_1 plots show that the error due to RF was dominant when RF size was large. We qualitatively and quantitatively proved that σ can be minimized by setting the RF size in a retinomorph neural network model consisting of nonidentical photodetectors to a nonzero value.

References

- [1] A. Utagawa, T. Asai, T. Sahashi and Y. Amemiya, "Stochastic resonance in retinomorph neural networks with nonidentical photoreceptors and noisy McCulloch-Pitts neurons," *Proceedings of NOLTA 2008*, pp. 124–127, 2008.
- [2] E. Simonotto, M. Riani, C. Seife, M Roberts, J. Twitty and F. Moss, "Visual Perception of Stochastic Resonance," *Phys. Rev. Lett.* vol. 78, no. 6, pp. 1186–1189, 1997.
- [3] K. Funke, N. J. Kerscher and F. Wörgötter, "Noise-improved signal detection in cat primary visual cortex via a well-balanced stochastic resonance like procedure," *European Journal of Neuroscience*, vol. 5, pp. 1–35, 2007.
- [4] P. C. Gailey, A. Neiman, J. J. Collins, and F. Moss, "Stochastic Resonance in Ensembles of Nondynamical Elements: The Role of Internal Noise," *Phys. Rev. Lett.*, vol. 79, no. 23, pp. 4701–4704, 1997.